JOURNAL OF AIRCRAFT
Vol. 42, No. 2, March–April 2005

Near Real-Time Simulation of Rotorcraft Acoustics and Flight Dynamics

Kenneth S. Brentner,* Leonard Lopes,† Hsuan-Nien Chen,‡ and Joseph F. Horn§
The Pennsylvania State University, University Park, Pennsylvania 16802

In this paper, a near-real-time rotorcraft flight dynamics-acoustics prediction system is presented. The high-fidelity PSU-WOPWOP rotor noise prediction code is coupled with the GENHEL flight simulation code, which provides low-fidelity blade loading and motion. This system is an initial step intended to investigate the feasibility of real-time rotorcraft noise prediction and to demonstrate the utility of such a system. Limited acoustic validation is shown for a contemporary-design four-bladed main rotor in level flight. A complex 80-s maneuver was used to demonstrate the potential of the coupled system. This realistic maneuver includes a climb, coordinated turn, and level flight conditions. The noise predictions show changes in main rotor noise radiation strength and directivity caused by maneuver transients, aircraft attitude changes, and the aircraft flight—but do not include the effect of blade-vortex-interaction noise. A comparison of the total noise with the thickness and loading noise components helps explain the noise directivity. The computations for a single observer were very fast, although the algorithm is not currently organized as a real-time computation.

Introduction

ROTORCRAFT noise is one of the key objections to the introduction of rotorcraft into commercial service in metropolitan areas. Existing operators are often burdened by the requirement to fly complex flight paths to avoid excessive noise exposure to neighboring communities. Much research has been performed over the past 20 years to understand the rotor noise generation and propagation, to develop prediction methodologies to aide regulatory bodies and rotorcraft manufacturers, and to help operators reduce noise. Even so, the rotor noise prediction problem requires a detailed understanding of the rotor aerodynamics and dynamics, which is still extremely challenging. In fact, most acoustics analysis codes only compute noise levels for trimmed flight conditions given a set of calculated or measured air loads. Such acoustics predictions have been successfully validated with carefully controlled wind-tunnel tests, but comparison with flight data is much less accurate.

Real rotorcraft flight is unlike steady-state flight predictions because it is typically not truly steady—gusts, atmospheric turbulence, and pilot-induced transients influence both the aircraft position, velocity, acceleration, and radiated noise. For these reasons very little first-principles-based prediction capability has been developed specifically for flight-path optimization for minimum noise. Flight testing and empirically based prediction models have been the primary tools used to formulate quiet flight procedures. Yet such a capability would be of great benefit to rotorcraft designers, operators, regulatory agencies, and land-use planners, provided it was relatively easy to use and not too computationally demanding. If such a system could operate in a real-time mode, then pilot-in-the-loop simulations could also be performed.

Recent work on the prediction of rotor noise in maneuvering flight has focused attention on the development of highly efficient acoustic algorithms for maneuver.[1,2] The rapid advance in computer processor power, innovations in parallel processing,[3] and improvements in the efficiency of numerical algorithms all have greatly increased the speed of calculation for noise prediction. Still, the complexity of the rotor aerodynamic, dynamic, and acoustic computations required in rotor noise prediction has made real-time implementation apparently impractical—even unthinkable.

But, what if the accuracy demands on a rotorcraft noise prediction system were relaxed somewhat to take into account the uncertainty that inevitably occurs in real flight conditions? If such an allowance were made, maybe then a combination of low-fidelity, first-principles methods and rotor airloads modeling could provide input data to a high-fidelity rotor noise prediction tool. Such a system is the ultimate goal of the work initiated in this paper.

Flight simulation codes are the main computational tool for rotorcraft flight dynamics analysis. These codes calculate the orientation and trajectory of a helicopter for specified pilot control inputs and atmospheric disturbances, often in a real-time environment. Over the last two decades, real-time models have come to include detailed representations of main rotor-blade loadings, rigid blade dynamics, and simplified dynamic inflow.[4] With the ever-increasing speed of microprocessors, the achievable level of fidelity has the potential of becoming quite high, including the possibility of full free-wake computation in the near future.[5]

This paper is a "first step" toward real-time rotorcraft noise prediction. The goal here is first to determine if it is feasible to perform acoustic computations in real time at reasonably high fidelity. The very idea of real-time rotor noise prediction is new, and such a tool could be very useful even if there were no first-principles approach to providing the rotor motion and loading data in real time. Such data might come from on-blade measurements or even ad hoc rotor loads modeling. Such modeling is not proposed in this paper, but the subject of later work. The second goal of this paper is to demonstrate that a low-fidelity loading model coupled with a high-fidelity noise prediction can provide insight into the maneuvering flight of rotorcraft. Validation of such a tool is extremely difficult and is beyond the scope of this initial paper. Rather if interesting effects can be demonstrated with a low-fidelity tool, this will provide motivation for more in-depth analysis of these effects with high-fidelity tools in the future.

Approach

The objective of this study is to investigate the feasibility and potential benefits of integrating rotorcraft noise prediction and flight dynamics simulation into a real-time or near real-time analysis

Received 24 July 2003; revision received 21 July 2004; accepted for publication 24 July 2004.

*Associate Professor, Department of Aerospace Engineering, 233D Hammond Building; ksbrentner@psu.edu. Senior Member AIAA.

†Graduate Research Assistant, Department of Aerospace Engineering, 143 Research West; lvl105@psu.edu. Student Member AIAA.

‡Graduate Research Assistant, Department of Aerospace Engineering, 143 Research West; huc115@psu.edu. Student Member AIAA.

§Assistant Professor, Department of Aerospace Engineering, 233G Hammond Building; joehorn@psu.edu. Senior Member AIAA.

code. The high-fidelity noise prediction code PSU-WOPWOP[1,2] (also known as WOPWOP3) has been mated with the flight simulation model GENHEL[4] to provide a flight dynamics and acoustics analysis of a utility transport helicopter. In the remainder of this paper, each of the components of this simulation system will be described, and the feasibility of a coupled, real-time prediction of rotorcraft flight dynamics and noise will be investigated.

GENHEL Flight Simulation Code

GENHEL is a nonlinear mathematical model of the flight dynamics of a utility helicopter. The code used in this study is based on the version maintained by the NASA/U.S. Army rotorcraft division. The simulation model includes a total force, large-angle representation of the six-degree-of-freedom rigid-body dynamics of the fuselage. Rigid flapping and lagging dynamics of the rotor blades are also included along with a three state Pitt–Peters dynamic inflow model. Dynamic models of the engine, rpm governor, and flight control systems are also included. This code is widely accepted by government and industry as a valid tool for analysis of flight dynamics and handling qualities.

The rotor model uses a blade element representation, in which the local velocities are calculated for a set of segments along each blade, and the aerodynamic loading is then calculated based on the local Mach number, angle of attack, and yaw angle of the flow. The tangential and normal components of aerodynamic loading along the blade as well as the blade location at each time step are computed by GENHEL. The rather simplistic aerodynamic modeling in GENHEL should provide the correct magnitude of the first few harmonics of the rotor loading, but it will not accurately predict the higher-frequency components of loading and will completely miss any impulsive loading such as blade-vortex interaction (BVI) or transonic flow effects.

An extensive validation program was conducted for the Army GENHEL simulation software.[6] The trim characteristics and dynamic response of the simulation model were compared to equivalent data from flight tests. Overall, basic aircraft parameters such as attitude, angular rate, and velocities showed good agreement with flight-test data, with some exceptions in the off-axis response. Detailed blade loading data were not evaluated in this validation study, but the aircraft response prediction gives some indication that the general characteristics of blade loads are captured by the model.

The code has been modified in this study to provide all of the parameters needed for noise prediction. In particular, the aircraft motion, individual blade motion, and loading are all provided to PSU-WOPWOP as a function of time. GENHEL was also modified to use an increased number of spanwise segments for the computation of blade loading. A maneuver controller (pilot model) has been added to the code to allow simulation of basic flight maneuvers in a non-real-time environment without a pilot in the loop. In non-real-time computations the code is capable of executing in a much shorter time than the actual maneuver, even on a desktop personal computer.

PSU-WOPWOP Noise Prediction Code

The PSU-WOPWOP code has been used to calculate rotor source noise in both steady and transient maneuvering flight. PSU-WOPWOP was specifically developed to predict rotor noise for a rotorcraft with multiple rotors flying an arbitrary flight path. The blade motion and loading are assumed to be independent and nonperiodic for each rotor blade. PSU-WOPWOP is a source-time-dominant implementation of Farassat's retarded-time formulation 1A (Ref. 7) of the Ffowcs Williams–Hawkings equation.[8] Although this is the same formulation as is used in the NASA WOPWOP[9] code, the source-time-dominant[10] approach was chosen because it was found to be the most efficient acoustics algorithm for the maneuver problem. The source-time-dominant approach computes the noise from each point on the rotor blade and determines when that signal will reach the observer. The arrival time (when the signal arrives at the observer location) is different for each source point; therefore, the acoustic pressure-time history from each source point must be interpolated to provide a signal at the desired observer time. Only then can the contribution from each point on the blade be summed to give the resultant acoustic pressure at the desired observer time. For future real-time implementation, this part of the algorithm requires modification. Using the source-time-dominant algorithm, PSU-WOPWOP runs approximately 50 times faster than the NASA version of WOPWOP modified for maneuver.

The code was developed with an object-oriented design. The result is a flexible code that can model the full geometrical complexity of any rotor configuration without modeling approximations used in other codes. All geometric details—such as hinge locations, rotor blade, and body motions—can be arbitrarily specified as user input. Currently only rigid blade motion is implemented.

In this work, PSU-WOPWOP's compact-chordwise option was used for loading noise predictions because it utilizes blade section forces rather than surface pressures; therefore, it is better suited for coupling with GENHEL. This approximation (described in Ref. 1) leads to some modeling error in the loading noise, but yields a dramatic reduction in loading noise computation time and is consistent with the low-fidelity loading inputs provided by GENHEL. PSU-WOPWOP is capable of predicting both BVI noise and high-speed impulsive (HSI) noise, but GENHEL is not capable of computing the needed aerodynamic data for these impulsive noise sources. When BVI noise is predominant, the high-frequency components of noise caused by the impulsive loading will not be predicted by the coupled flight simulation—noise prediction system. Even so, the low-frequency rotational noise (nonimpulsive noise) from the current prediction system should be accurately predicted. A more complete description of the PSU-WOPWOP code can be found in Refs. 1, 2, 11, and 12.

Coupled Acoustics—Flight Simulation System

The integration of PSU-WOPWOP with GENHEL enables a seamless transfer of flight dynamic data into the noise prediction analysis. In the initial phase of the system development, the coupling between the codes is a loose, one-way coupling. Presently, the maneuver is first run in the GENHEL code, which determines the flight dynamics and rotor blade loading. PSU-WOPWOP uses this data to predict the noise. This implementation is not suitable for real-time predictions, but is adequate to evaluate both the fidelity issues and potential for real-time noise prediction. Although GENHEL loading is only useful for low-frequency loading noise predictions, it should provide sufficiently accurate blade motions for maneuver thickness noise prediction. The GENHEL flight path and pilot control predictions will also be extremely helpful in setting up a higher-fidelity comprehensive analysis.

Aircraft Description

The aircraft investigated in this study is representative of a utility transport helicopter. It is a single-rotor/tail-rotor configuration with an articulated horizontal stabilizer. The main rotor is a four-bladed articulated rotor with swept blade tips. The main rotor-blade planform is shown in Fig. 1. The tail rotor is modeled using a simplified Bailey solution in GENHEL; hence, individual blade motion and loading are not modeled. For this reason the tail rotor has not been included in noise predictions. However, in the future the simulation could be upgraded to include a blade-element tail rotor model in order to include tail rotor noise in the analysis. The aircraft includes basic electronic stability augmentation in the roll, pitch, and yaw axes. To simulate basic maneuvers without a pilot in the loop, an outer-loop controller was designed and implemented. A description of key aircraft parameters used in the coupled acoustics–flight simulation system predictions is given in Table 1.

Fig. 1 Main rotor-blade planform of utility transport helicopter used in coupled acoustic–flight dynamics computations.

Table 1 Description of utility transport helicopter used in current study

Parameter	Value
Aircraft weight	74.84 kN
Rotor radius	8.18 m
Nominal rotor speed	258 rpm
Radius of tip sweep	95%
Tip sweep angle	20 deg

Acoustic Signal Processing

Two types of acoustic predictions have been made in this paper: acoustic pressure time history and overall sound pressure level (OASPL). The acoustic pressure is the fundamental type of acoustic prediction; OASPL is derived through a spectral analysis of the acoustic pressure signal. The acoustic pressure computations presented only include the frequency components between 5 and 200 Hz. Although predicted acoustic signals often have some content below 5 Hz (i.e., a slowly varying mean level), a microphone typically does not measure these frequencies; hence, it is removed from prediction so as not to contaminate the SPL levels. The 200-Hz high-frequency limit had essentially no impact on the predictions because only low-frequency input data from GENHEL are used.

OASPL values are not representative of human perception nor are they typically used in certification measurements, but they do characterize the low-frequency content of the acoustic signals predicted with the present acoustic/flight dynamics simulation. If A-weighted SPL or perceived-noise-level metrics had been used, an emphasis would have been place on the portion of the spectrum known to be in error. The OASPL values were computed by applying a Hanning window to a 0.5-s segment of the acoustic pressure time history. A 4.26-dB broadband correction factor[13] was then added to the OASPL level to compensate for the effect of the Hanning window on the total signal power. [A Hanning window is applied because the signal is not periodic, but the application of the Hanning window results in a loss. For a broadband signal the resultant spectral density must be multiplied by a factor of $\sqrt{(8/3)}$, that is, an addition of 4.26 dB (Ref. 13).]

Validation of Coupled Acoustics–Flight Simulation System

Whenever a new computational methodology or procedure is developed, it is critical that the end-to-end process be validated to the maximum extent possible. Such a validation process is extremely difficult in the case of maneuvering rotorcraft noise prediction. The difficulties come from several sources. First, very few noise measurements of rotorcraft during maneuvering flight exist, and it is impractical (if not impossible) to perform such measurements in a wind tunnel. Second, if flight measurements were available, all noise sources would be present in the acoustic measurements: engine noise, tail rotor noise, and the main rotor noise. Pilot input transients, wind gusts, and atmospheric turbulence would also influence the measured noise. Finally, many of the datasets that have been taken are not openly available. Nevertheless, some validation of the coupled GENHEL–PSU-WOPWOP system is still possible.

Variation of Spatial and Temporal Resolution

The first validation performed on the coupled GENHEL–PSU-WOPWOP system was an internal consistency check. In a typical GENHEL computation, the blade is divided up into five radial segments, and the time integration is performed at 0.01-s intervals (approximately 15.5-deg azimuth steps). This spatial and temporal discretization is very coarse by acoustic standards; hence, these parameters were investigated. A minor modification was made to GENHEL to allow a significantly higher number of radial stations (e.g., up to 30 segments were investigated in this study). The effect of number of blade segments used in GENHEL was investigated for the utility transport aircraft flying in level flight at a velocity of 41.16 m/s.

Figure 2 shows how the predicted spanwise-loading distribution changes when the number of blade segments was increased from 5 to 10, 20, and 30. As the number of blade segments increased, the details of the loading distribution changed slightly, especially near the tip of the rotor blade. The largest changes in loading are seen when increasing from 5 to 10 and from 10 to 20 blade segments. The variation in the spanwise loading for the particular azimuth angle used in Fig. 2 is typical. Figure 3 shows a similar comparison for when the integration time-step size used in GENHEL is reduced from the typical value of 0.01 s to a smaller value 0.005 s. Again only a small change is evident in the blade loading. (Smaller integration time steps are not currently practical in GENHEL.) Although not shown, either an increase in number of blade segments or decrease in integration time-step size had relatively small effect on the global quantities computed by GENHEL, such as rotor thrust, blade motion, and aircraft trajectory.

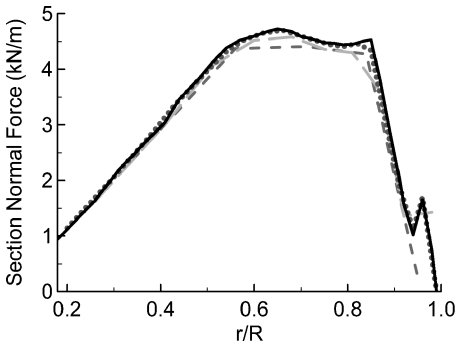

Fig. 2 Section normal force for blade 1 at azimuth angle of 23 deg (t = 1.2 s) plotted as a function of span for different numbers of GENHEL blade segments: - - -, 5 segments; – – –, 10 segments; · · · ·, 20 segments; and ——, 30 segments.

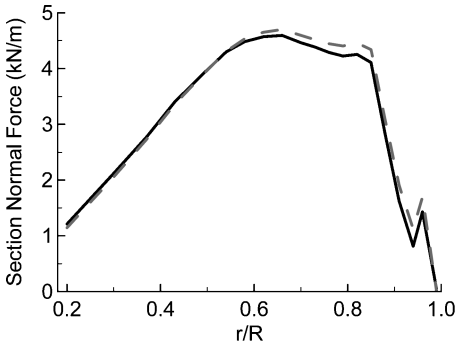

Fig. 3 Section normal force for blade 1 at azimuth angle of 23 deg (t = 1.2 s) plotted as a function of span for different GENHEL time-step sizes: - - -, $\Delta\tau$ = 0.01 s; and ——, $\Delta\tau$ = 0.005 s.

The effects of these variations in loading spatial and temporal resolution on the predicted acoustic pressure signature are shown in Fig. 4. Figure 4a shows the acoustic pressure-time history prediction, together with the thickness and loading components, for an observer 30.48 m directly below the helicopter at $t = 2.0$ s. Notice that at the beginning of the time history the acoustic pressure is dominated by the thickness noise, but as the helicopter approaches the observer, the loading noise component becomes dominant (as expected). The thickness noise prediction for three different spatial resolutions was used to compute the thickness noise—grids with 10×10, 20×20, and 30×30 panels on both the upper and lower surfaces—are shown for a segment of the time history in Fig. 4b. There is very little difference between the three predictions, although the lowest resolution does vary slightly from the others. The temporal resolution used in the thickness noise computation (which is independent from that used in the loading noise prediction) is varied for the same time segment in Fig. 4c. A small phase shift is evident in the comparison, but the waveform shape is essentially unchanged. Similar comparisons of the loading spatial and temporal resolution effect on loading noise prediction are shown in Figs. 4d and 4e. Only the lowest number of loading segments (5) is noticeably different,

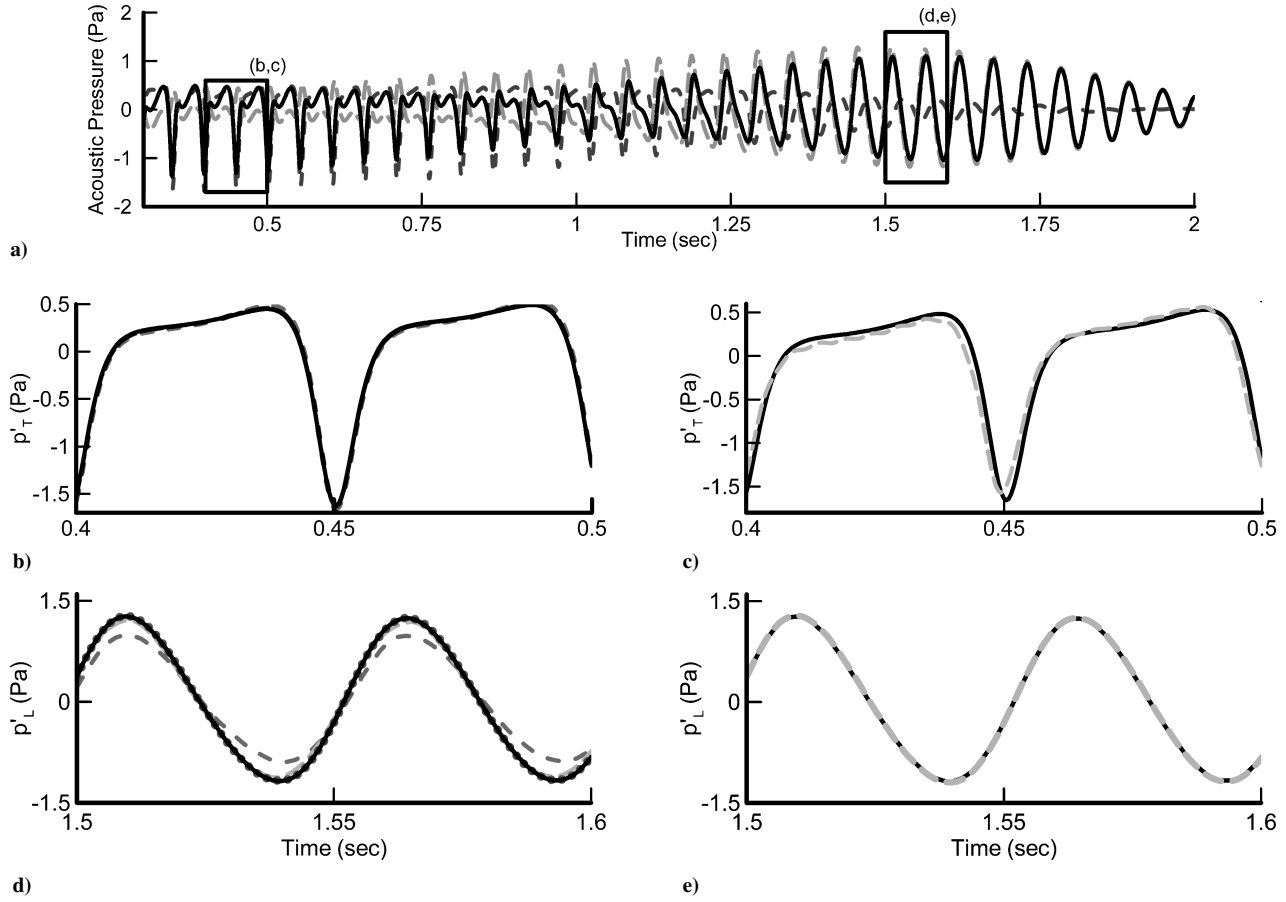

Fig. 4 Acoustic pressure plotted as a function of time for helicopter flying 41.16-m/s level flight. The observer is 30.48 m below the helicopter at t = 2.0 s: a) - - -, thickness, – – –, loading, and ——, total acoustic pressure at the highest spatial and temporal resolutions; b) comparison of thickness noise for - - -, 10 × 10 grid, – – –, 20 × 20 grid, and ——, 30 × 30 grid resolutions; c) comparison of thickness noise for – – –, $\Delta\tau$ = 0.01 s and ——, $\Delta\tau$ = 0.005 s; d) comparison of loading noise using - - -, 5 segments, – – –, 10 segments, · · · ·, 20 segments, and ——, 30 segments; and e) comparison of loading noise using – – –, $\Delta\tau$ = 0.01 s and ——, $\Delta\tau$ = 0.005 s.

indicating that the loading noise computation at this resolution is not converged. The two different time steps used to compute the loading noise in Fig. 4e yield essentially identical results. Such large time steps are allowable only because the blade loading does not have any significant high-frequency content. Based on these results, a set of 10 × 10 grids (upper and lower surfaces) was used for thickness noise computations with a integration time step (source time) of 0.005 s. For the loading noise computations, 10 segments were used with an integration time step in GENHEL of 0.01 s.

Comparison with Wind-Tunnel Data

There are very little data available to validate the noise of rotorcraft in maneuvering flight. Nonetheless, it is important to demonstrate that the GENHEL–PSU-WOPWOP system can predict noise accurately for steady flight cases. For this purpose, experimental data from a wind-tunnel test in the German-Dutch Wind Tunnel (DNW) was chosen for comparison. The experimental setup and test are described, followed by a comparison of predicted and measured noise at two microphone locations for two flight conditions.

Experiment Description

A $\frac{1}{5}$-scale United Technologies Corporation contemporary design, four-bladed, pressure-instrumented main rotor was tested while several microphones recorded the noise generated by the rotor.[14] The main rotor airloads and noise were measured at various advancing-tip Mach numbers. The rotor was trimmed to zero blade flapping, but the lag motion during the test was not reported. The rotor test was focused on measuring noise in both BVI and HSI noise conditions, precisely the conditions in which the GENHEL–PSU-WOPWOP system cannot accurately predict noise. Nevertheless, two microphone locations (microphone 1 and 7 in Ref. 14) did not include significant BVI or HSI noise; hence, these two microphones are adopted as observer locations in the noise predictions. Microphone 1 was located in front of the rotor along the rotor centerline (180-deg azimuth angle). Microphone 7 was also located in the rotor plane 30 deg from the centerline microphone (150 deg in rotor azimuth angle) on the advancing side. Both in-plane microphones are located three rotor radii from the rotor hub. A schematic of the test setup is shown in Fig. 5. The rotational tip Mach number is $M_H = 0.636$ (Ref. 15). To focus on the thickness and loading noise prediction, level flight conditions were chosen with advancing-tip Mach numbers $M_{AT} = 0.690$ and 0.796, respectively. With these selections, the influence of any BVI or HSI noise was minimized.

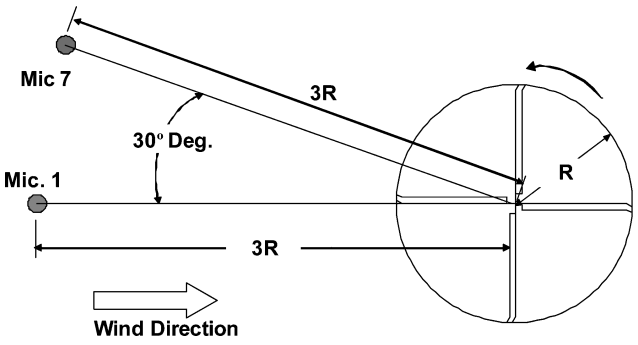

Fig. 5 DNW experiment setup.

The GENHEL flight simulation code is designed to compute the flight dynamics of a full-scale utility helicopter—NOT an isolated rotor in a wind tunnel. The rotor was modeled at full scale in the GENHEL simulation. Simulated level forward flight with a constant forward speed of 15.4 and 51.7 m/s and a constant rotation rate of 258 rpm resulted in the desired advancing-tip Mach numbers of $M_{AT} = 0.690$ and 0.796. In the GENHEL simulation, all rotorcraft degrees of freedom were allowed, but in level trimmed forward flight the rotorcraft attitudes are essentially constant throughout the simulation. The GENHEL simulation predicted some blade flapping (very small), but this was set to zero in the PSU-WOPWOP noise prediction so that the prediction would represent the test more accurately. In effect, only the rotor speed, blade pitch, and appropriately scaled blade loading data from GENHEL were used in the PSU-WOPWOP noise prediction.

Case 1: $M_{AT} = 0.690$

When the advancing-tip Mach number is $M_{AT} = 0.690$, there is no shock generated on the blade surface, and therefore HSI noise is not expected in the measured results. However, the measured data contain a small amount of BVI noise for both microphones 1 and 7. [BVI noise can be identified as the narrow impulse(s) just prior to the large negative peak, which is primarily thickness noise.] Figure 6 shows that the predicted total acoustic pressure matches the experimental data at microphone 1 very well, although there is a slight variation between blades that can be seen in the data. In this case the noise is dominated by thickness noise, but loading noise is present, contributing about 20% of the total acoustic pressure amplitude. (Individual thickness and loading noise components are not shown.) A comparison of predicted and measured noise at the location of microphone 7 is shown in Fig. 7. Again the noise is predominantly thickness noise, but the measured acoustic pressure history also contains more BVI than microphone 1. At microphone 7 the agreement between prediction and data are not as good that obtained for microphone 1—the total acoustic pressure magnitude is less than the DNW measured value—but the agreement is still satisfactory.

Case 2: $M_{AT} = 0.796$

As the advancing-tip Mach number is increased to $M_{AT} = 0.796$, it is observed from the experimental data that there is still no significant shock-generated noise even though the amplitude of the acoustic pressure signal is two to three times that of the earlier case (see Figs. 8 and 9). For this flight condition, there is now a significant set of BVI impulses in the acoustic pressure history at the microphone 1 location. The PSU–WOPWOP prediction for this condition agrees well in both the shape and amplitude of the acoustic pressure signature, except for the BVI impulses. The acoustic pressure negative peak is somewhat overpredicted, but otherwise is in good agreement. In fact the agreement between the prediction and the data from some blades is slightly better than others.

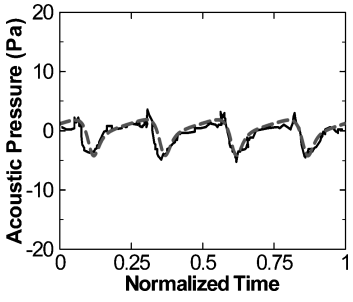

Fig. 6 Acoustic pressure comparison at microphone 1 for one rotor revolution, M_{AT} = 0.690: ——, experiment (Ref. 14); and – – –, prediction.

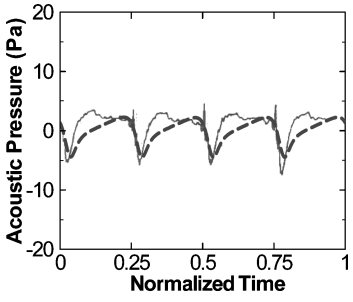

Fig. 7 Acoustic pressure comparison at microphone 7 for one rotor revolution, M_{AT} = 0.690: ——, experiment (Ref. 14); and – – –, prediction.

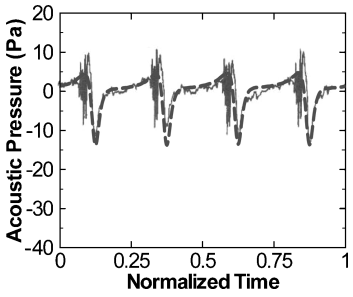

Fig. 8 Acoustic pressure comparison at microphone 1 for one rotor revolution, M_{AT} = 0.796: ——, experiment (Ref. 14); and – – –, prediction.

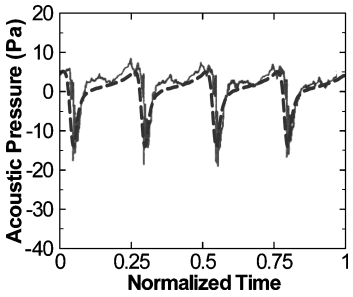

Fig. 9 Acoustic pressure comparison at microphone 7 for one rotor revolution, M_{AT} = 0.796: ——, experiment (Ref. 14); and – – –, prediction.

Overall, the results shown in Figs. 6–9 demonstrate that the coupled GENHEL–PSU-WOPWOP system prediction matches the experimental data quite well for both forward flight speeds and microphone locations. When BVI occurs, it is not predicted, but the underlying acoustic pressure signal has both the correct shape and amplitude. Further validation out of the rotor plane would be useful, but these results give some confidence in accuracy of the coupled flight dynamics–rotor noise prediction system.

Complex Maneuver Demonstration

A complex maneuver, typical of a routine operation, has been used to demonstrate the capability of the coupled system and to investigate the potential for real-time rotorcraft noise prediction.

Description of Maneuver

The maneuver investigated is representative of a takeoff and climb-out followed by a coordinated turn. The aircraft starts in 20.58-m/s level flight just above the ground. The aircraft then initiates a 5.08-m/s climb and simultaneously accelerates to 51.44-m/s forward airspeed. When the aircraft reaches 60.96 m altitude, it levels off and performs a 180-deg coordinated turn, at constant airspeed and altitude. The turn is performed using a 28-deg bank angle and a load factor of about 1.15. The aircraft finishes the maneuver in straight-and-level flight. The entire time for the maneuver is 80 s.

Figure 10 shows a three-dimensional plot of the vehicle trajectory. Figure 11 shows time histories of the pilot control inputs and the aircraft response. Although the aircraft is in quasi-steady equilibrium flight for much of the maneuver, this analysis also includes the transient effects that occur during the transitions between the various phases of the maneuver. For example, transient dynamics occur at the initiation of the climb, the termination of the climb, the initiation of the turn, and the termination of the turn. These transients are a result of the helicopter dynamics and the specific control inputs from the pilot model trying to achieve the desired flight states.

Some sense of the variation of rotor loading with time is given in Fig. 12. In this figure, the section normal force for blade 1 is plotted as a function of radius and rotor azimuth for several selected times during the flight. (The time indicates the beginning of a revolution.) A great deal of information is found by looking at the rotor loading as a function of time. In particular, Fig. 12 shows, among other things, that at completion of the climb phase ($t \approx 14$ s) when the collective pitch is reduced, the normal force over the rotor disk is temporarily

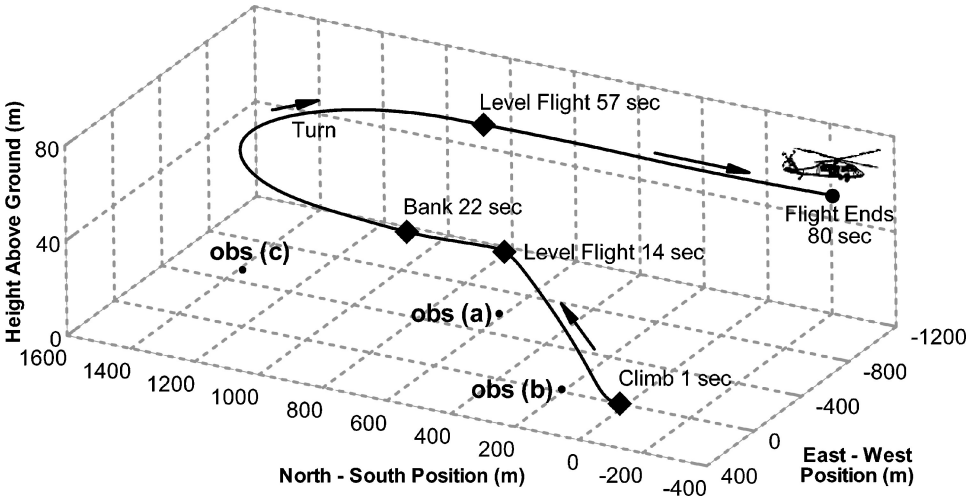

Fig. 10 Flight trajectory for complex maneuver.

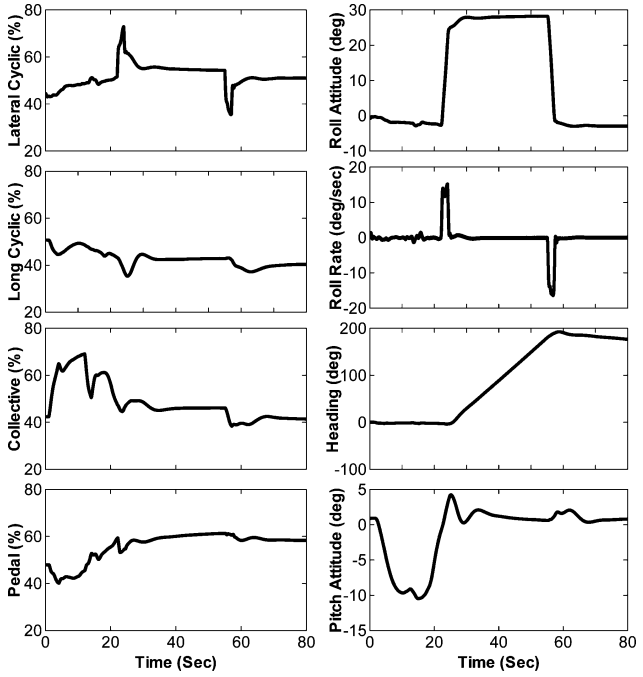

Fig. 11 Pilot control inputs and aircraft response for complex maneuver.

smaller than the aircraft weight. Other transient changes in loading can be seen after the helicopter enters the turn at $t \approx 25$ s and as it leaves the turn at $t \approx 57$ s.

Maneuver Noise Predictions

Although it is difficult to completely characterize the noise for an 80-s maneuver, in this section the OASPL will be shown both for a few individual observer locations as a function of time and as the directivity over a large area for a few selected times.

Noise at Isolated Observers Positions

Three separate observer positions were selected to show how the noise level changed throughout the 80-s maneuver. Acoustic pressure-time histories are not shown because there are simply too many waveforms to present in an 80-s time period. OASPL values are plotted as a function of time in Fig. 13 for each of the three observer positions shown indicated in Fig. 10. The total noise, thickness noise, and loading noise components are each shown. Notice that for each of the histories there are fairly rapid changes in the OASPL levels, even though the OASPL is an integration over 0.5 s of acoustic data. These rapid changes are related to both the transient changes in aircraft loading and attitude. Although the loading noise is the dominant noise source much of the time at these three locations, each time history has some period of time when the thickness noise is the dominate source.

Noise Directivity

Determination of the noise directivity over a large area is important to understand the full impact of the radiated rotor noise. The OASPL level has been computed on a 2000 m $\times$ 1600-m grid corresponding to the ground plane shown in Fig. 10. The measurement locations were spaced 20 m apart in each direction, resulting in 8181 total measurement points. The OASPL contours were computed at 1-s intervals for the entire 80-s maneuver.

Figure 14 shows the OASPL pressure level for several time steps during the maneuver. The small black circle in each of the contour plots indicates the location of the helicopter at the specified time. The circle radius is four times the radius of the helicopter main rotor. The specific times were chosen to display key events in the flight. At $t = 7$ s, the aircraft is in the middle of the initial climb. At $t = 14$ s, the aircraft has reached the flight altitude, and the collective pitch is reduced. At this time the shape of the noise contours has changed slightly and become more complex. The contour at $t = 21$ s is just before the aircraft enters the coordinated turn while $t = 25$ s is a few seconds after entering the coordinated turn. Notice at $t = 28$ s the most intense noise region has shifted to the advancing side of the helicopter, and the shape of the intense region is more narrow and elongated. This is related to the aircraft roll angle (28 deg) during the turn. Throughout the turn, the helicopter is in quasi-steady equilibrium, and the noise contour on the ground is essentially the same except that it follows the aircraft as it turns. This can be seen by comparing the $t = 28$, 42, and 56 s contours. At $t = 57$ s, the aircraft leaves the turn and levels out. The aircraft then enters straight-and-level flight, and the radiation levels ahead and on the advancing rotor side of the aircraft generally increase even though the peak level decreases slightly. This is seen in the $t = 60$ and 65 s contours. The contours for times greater than 65 s are not shown, but are similar to the $t = 65$ case. Although Fig. 14 generally characterizes the maneuver, there is a great deal of complexity that requires more in depth analysis (which is beyond the scope of this paper).

Comparison of Thickness and Loading Noise

One way in which the results of Fig. 14 can be understood more clearly is to examine the constituent noise sources separately. To do this, loading and thickness noise overall sound pressure levels are shown in Figs. 15 and 16, respectively. By comparing all three figures (14–16), it is apparent that both loading and thickness noise

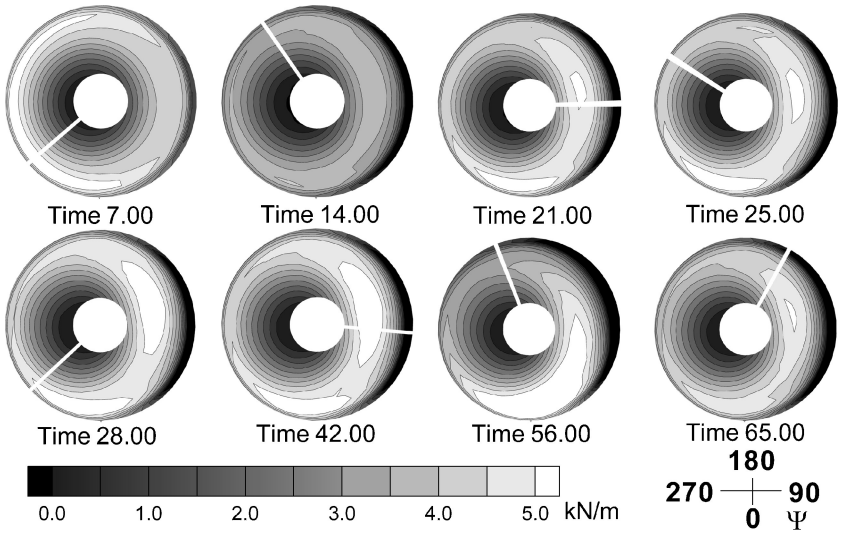

Fig. 12 Normal-force distribution for blade 1 for selected times during the complex maneuver. Note: these plots are not uniformly distributed in time.

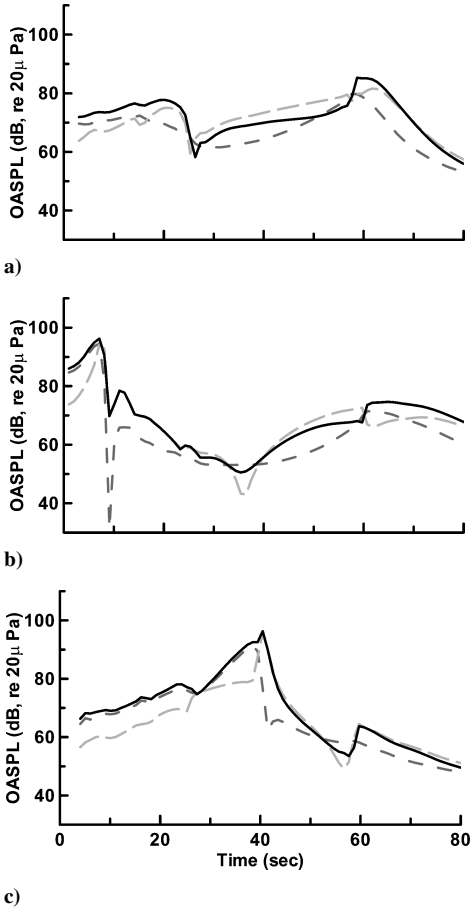

Fig. 13 Overall sound pressure level for the complex maneuver plotted as a function of time. The components of noise are shown as - - -, thickness noise; – – –, loading noise; and ——, total noise. Each subplot is a different observer location shown in Fig. 10: a) x = (609, −609, 0) m; b) x = (200, 0, 0) m; and c) x = (1350, −500, 0) m.

sources are significant in some regions on the ground. For instance, during the climb ($t = 7$ s) loading noise is dominant; however, thickness noise contributes to the higher level contours during the turn-and-level flight. As might be expected, the directivity of the higher intensity regions are somewhat different for thickness and loading noise—loading noise tends to radiate more to the right and left of the vehicle, whereas thickness noise radiates primarily forward on the advancing-rotor side of the aircraft.

Table 2 GENHEL execution time for 80-s maneuver (CPU seconds)

$\Delta\tau$	10 segments	20 segments	30 segments
0.01	0.70	0.93	1.18
0.005	1.40	1.85	2.36

Consideration of Real-Time Noise Prediction

The final area of study and principal goal of this paper is to consider the feasibility of real-time noise prediction using the coupled GENHEL–PSU-WOPWOP system. GENHEL is already used for real-time flight simulations, and so here the main interest is how fast the PSU-WOPWOP code can compute the noise at a single observer location. The 80-s complex maneuver is used as the test case for this assessment. Although the codes are only loosely coupled at present, it is expected that the execution time for each component is representative of that in a tightly coupled real-time system. Timings have been performed on a 3.4-GHz Pentium 4 processor configured with an 800-MHz front-side bus, 1 GB of system memory, and the Linux operating system (SUSE 9.1 with 2.6 kernel). The I/O time for both codes is not included because disk I/O would be avoided during a real-time execution. Although the machine was not operating in any type of real-time mode, the computer was dedicated to the prediction during the timing.

In Table 2 the execution time of the GENHEL computation for the 80-s complex maneuver is shown for two different integration time steps $\Delta\tau$ and 10, 20, or 30 loading segments. Each of these loading distributions was shown to be adequate in the present analysis in Fig. 2. As expected, GENHEL does not require much time to perform the computations—in the longest case (30 segments and $\Delta\tau = 0.005$ s) the GENHEL execution time is approximately 2.9% of the total maneuver time. For the minimum time case used for most of the computations in this paper (10 segments and $\Delta\tau = 0.01$ s), the execution time is only 0.88% of the time required for the actual maneuver.

A similar comparison is made for the PSU–WOPWOP thickness and loading noise calculations in Tables 3 and 4, respectively. Although GENHEL does not predict the mid- and high-frequency loading content, it is true in general that the blade loading temporal resolution will be higher than that for thickness noise. In fact, to accurately capture BVI noise the temporal resolution of the loading should be approximately 1 deg of rotor azimuth or less. In light of this, three integration step sizes are shown in Table 3: $\Delta\tau = 0.005$ s (approximately 15.5 deg azimuth); $\Delta\tau = 0.0006464$ s (approximately 4 deg azimuth); and $\Delta\tau = 0.0002586$ s (approximately 1 deg azimuth) for 10, 20, and 30 loading segments. The loading noise computations for the two lower $\Delta\tau$ cases are well below the 80 s required by the aircraft to complete the maneuver, even if 30

Table 3 PSU-WOPWOP execution time to compute loading noise for 80-s maneuver (CPU seconds)

$\Delta\tau$	10 segments	20 segments	30 segments
0.005	1.52	3.74	4.45
0.0006464	23.9	29.3	35.2
0.0002586	96.3	167	392

Table 4 PSU-WOPWOP execution time to compute thickness noise for 80-s maneuver (CPU seconds)

$\Delta\tau$	10×10	20×20	30×30
0.005	15.2	47.7	102
0.0006464	97.8	284	708

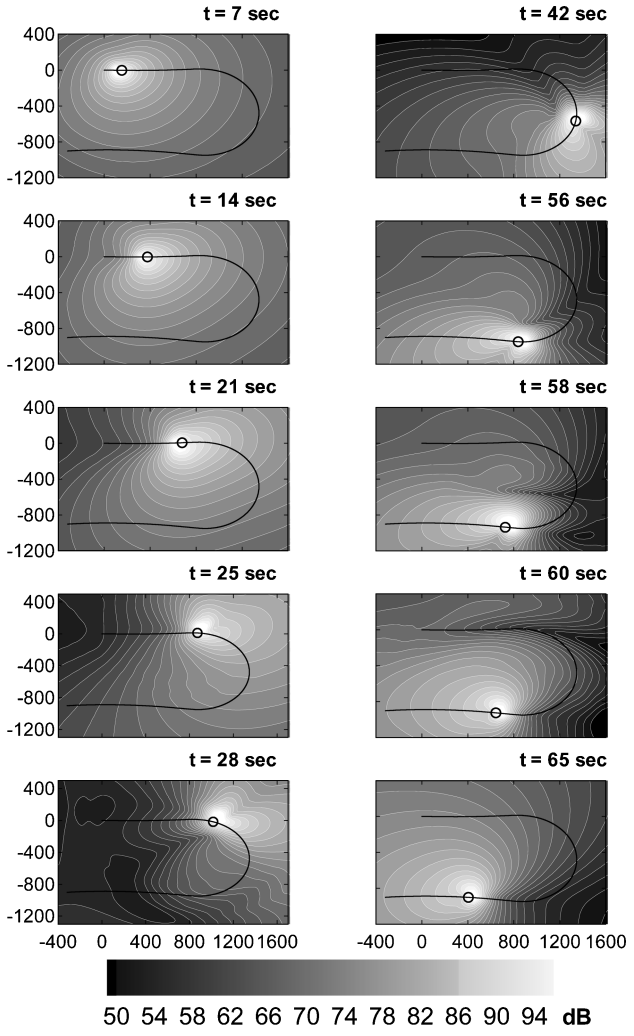

Fig. 14 Overall sound pressure level contours for the complex 80-s maneuver: ——, flight path; and ○, location of the helicopter. Spatial coordinate axes are specified in meters.

loading segments are used. The execution time for the smallest time step is only slightly longer than the maneuver for 10 segments and nearly five times as long as the maneuver when 30 segments are used.

The thickness noise computation time, shown in Table 4, is shown for three different grid resolutions—10×10, 20×20, and 30×30—both for the upper and lower surface grids. Note that the temporal resolution of thickness noise is not normally as high as that required by a high-fidelity loading noise computation; hence, only the two larger integration time steps $\Delta\tau$ are considered. If high grid resolution is required, the current approach will not be adequate for real-time computation (on a single processor). Yet, the

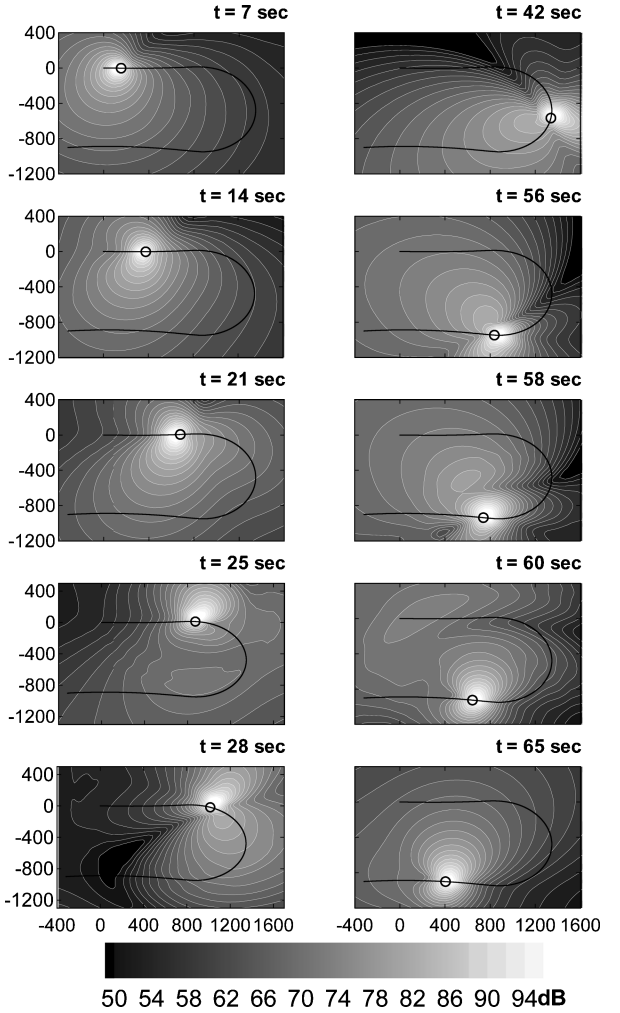

Fig. 15 Loading noise overall sound pressure levels for the complex 80-s maneuver: ——, flight path; and ○, location of the helicopter. Spatial coordinate axes are specified in meters.

grid-resolution study presented in Fig. 4 indicates that for this rotor and flight condition the 10×10 grid is sufficient for a converged thickness noise computation. Even the 20×20 grid can be used with the largest integration step size ($\Delta\tau = 0.005$ s) in less than 59.3% of the total maneuver time.

Now if the total execution time is considered (i.e., the sum of GENHEL, PSU-WOPWOP loading noise, and PSU-WOPWOP thickness noise), the results are quite encouraging. For the runs in this paper (10 loading segments with $\Delta\tau = 0.01$ s, and 10×10 thickness grid with $\Delta\tau = 0.005$ s), the computation time for a single observer is approximately 17 s for the 80-s maneuver. Clearly with gains in processor speed expected in the future, the total noise prediction might be faster than the maneuver time even for higher temporal and spatial resolution—without modification to the code. This is not to imply that first-principle-based high-fidelity rotor airloads computations will be this fast. But these results demonstrate that the full, high-fidelity acoustic prediction should be possible in a real-time prediction, and it might be worthwhile to develop medium-fidelity models of rotor airloads that are fast.

Waiting for faster processors is not the only or even the best approach to gaining further speed for real-time predictions. One alternative is to take advantage of the inherently independent nature of the computations in PSU-WOPWOP. Because numerical integration is a linear operation, the integration over each of the blade surfaces could easily be done in parallel. Some extra time would be required for message passing, but this should be minimal. Sufficient speedup could probably be gained just by performing the noise computation for each blade independently (for this rotor roughly a four-fold speedup). Parallelization could be taken even farther if

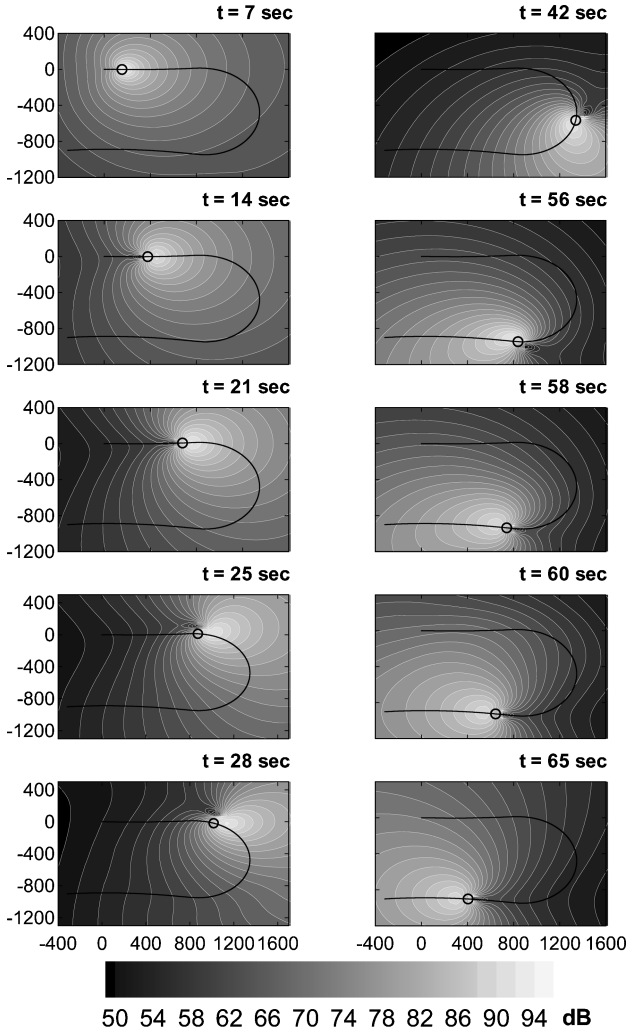

Fig. 16 Thickness noise overall sound pressure level contours for the complex 80-s maneuver: ——, flight path; and ○, location of the helicopter. Spatial coordinate axes are specified in meters.

needed by breaking the problem up into upper an lower surfaces, blade segments, etc.—all of which would be sent to different processors in a parallel computation. Airloads and rotor wake calculations could also benefit from parallel implementations. Another alternative would be to reformulate the thickness noise computation to be more efficient, as was done for compact-loading noise. Such a reformulation can have some error associated with it, but this might be acceptable given the level of fidelity in the rest of the system. In any case, with some algorithm reorganization real-time noise prediction is feasible within the framework of the coupled GENHEL–PSU-WOPWOP system.

Summary

In this paper, a near-real-time flight dynamics–acoustics prediction system has been presented. Although limited options are available for an end-to-end validation of the system, comparisons with wind-tunnel acoustic measurement are quite good for the thickness noise dominated in-plane observer positions. Modifications were made to the GENHEL model to increase temporal and spatial resolution. This did not adversely affect the flight dynamics model, and this change had a relatively small impact on execution time. The rotor loads computed by GENHEL's blade-element model with dynamic inflow is recognized not to have the mid- and high-frequency details needed for accurate loading noise prediction. Nevertheless, the low-frequency components of loading noise are expected to be reasonable. Thickness noise is relatively unaffected by the low-fidelity loading. This system is viewed as an initial configuration with the primary goal of assessing the possibility of real-time noise prediction in maneuvering flight.

A complex 80-s maneuver was used to demonstrate the potential of the coupled GENHEL–PSU-WOPWOP system. The noise prediction showed changes in noise strength and directivity caused by both transients in the maneuver and aircraft attitude changes. A comparison of the total noise with the thickness and loading noise components is useful to explain the source of the noise patterns. Although these computations do not provide the frequency range needed for typical noise metrics, they do have evidence of transients that are interesting and should be studied with a higher-fidelity blade loading.

The primary goal of this paper was achieved. The computations show that the noise prediction for maneuvering flight can be performed in less time than the maneuver. This is a rather remarkable accomplishment considering that reasonable spatial and temporal resolutions were used for both thickness and loading noise. In fact, the results indicate that somewhat high resolutions can be used and still achieve execution times less that the maneuver. Algorithm improvements, computation parallelization, and advances in computer processing speed all ensure that enough time is available for higher-fidelity predictions. Furthermore, these results provide motivation to take the next step of reorganizing the acoustic integration algorithm into a real-time algorithm. These results also demonstrate that it would be beneficial to develop a fast rotor loads model that would provide approximate BVI loading during maneuvering flight. If such a model were available, then real-time rotorcraft noise prediction would be able to reach its potential.

References

[1]Brès, G. A., Brentner, K. S., Perez, G., and Jones, H. E., "Maneuvering Rotorcraft Noise Prediction," *Journal of Sound and Vibration*, Vol. 275, No. 3–5, 23 Aug. 2004, pp. 719–738.

[2]Brentner, K. S., Perez, G., Brès, G., and Jones, H. E., "Toward a Better Understanding of Maneuvering Rotorcraft Noise," American Helicopter Society, Alexandria, VA, 2002.

[3]Long, L. N., and Brentner, K. S., "Self-Scheduling Parallel Methods for Multiple Serial Codes with Application to WOPWOP," AIAA Paper 2000-0346, Jan. 2000.

[4]Howlett, J., "UH-60A BLACK HAWK Engineering Simulation Program: Volume I—Mathematical Model," NASA CR-177542, USAAVSCOM TR 89-A-001, Sept. 1989.

[5]Quackenbush, T. R., Wachspress, D. A., Keller, J. D., Boschitsch, A. H., Wasileski, B. J., and Lawrence, T. H., "Full Vehicle Flight Simulation with Real Time Free Wake Methods," *American Helicopter Society Aerodynamics, Acoustic, Test and Evaluation Specialists Meeting*, American Helicopter Society, Alexandria, VA, Jan. 2002.

[6]Ballin, M. G., "Validation of a Real-Time Engineering Simulation of the UH-60A Helicopter," NASA-TM-88360, Feb. 1987.

[7]Farassat, F., and Succi, G. P., "The Prediction of Helicopter Discrete Frequency Noise," *Vertica*, Vol. 7, No. 4, 1983, pp. 309–320.

[8]Ffowcs Williams, J. E., and Hawkings, D. L., "Sound Generation by Turbulence and Surface in Arbitrary Motion," *Philosophical Transactions of the Royal Society, London, Series A*, Vol. 264, No. 1151, May 1969, pp. 321–342.

[9]Brentner, K. S., "Prediction of Helicopter Discrete Frequency Rotor Noise—A Computer Program Incorporating Realistic Blade Motions and Advanced Acoustic Formulation," NASA TM 87721, Oct. 1986.

[10]Brentner, K. S., "Numerical Algorithms for Acoustic Integrals with Examples for Rotor Noise Prediction," *AIAA Journal*, Vol. 35, No. 4, 1997, pp. 625–630.

[11]Bres, G. A., "Modeling the Noise of Arbitrary Maneuvering Rotorcraft: Analysis and Implementation of the PSU-WOPWOP Noise Prediction Code," M.S. Thesis, Dept. of Aerospace Engineering, Pennsylvania State Univ., University Park, May 2002.

[12]Perez, G., "Investigation of the Influence of Maneuver on Rotorcraft Noise," M.S. Thesis, Dept. of Aerospace Engineering, Pennsylvania State Univ., University Park, June 2002.

[13]Bendat, J. S., and Persal, A. G., *Engineering Applications of Correlation and Spectral Analysis*, 2nd ed., Wiley, New York, 1993, pp. 75, 76.

[14]Visintainer, J. A., Marcolini, M. A., Burley, C. L., and Liu, S. R., "Acoustic Predictions Using Measured Pressures From a Model Rotor in DNW," *Journal of the American Helicopter Society*, Vol. 38, No. 3, 1993, pp. 35–44.

[15]Lorber, P. F., "Blade-Vortex Interaction Data Obtained from a Pressure-Instrumented Model UH-60A Rotor at the DNW," *Journal of the American Helicopter Society*, Vol. 38, No. 3, 1993, pp. 26–34.